Nonlinear waves with negative phase velocity

Xiaoqing Huang,[1] Xuhong Liao,[1] Xiaohua Cui,[1] Hong Zhang,[2] and Gang Hu[1,*]
[1]*Department of Physics, Beijing Normal University, Beijing 100875, China*
[2]*Zhejiang Institute of Modern Physics and Department of Physics, Zhejiang University, Hangzhou 310027, China*
(Received 9 October 2008; revised manuscript received 19 May 2009; published 22 September 2009)

Recently, waves propagating with negative phase velocity [simply called antiwaves (AWs)] have attracted great attention in the area of nonlinear oscillatory systems. In the present work we investigate the parameter conditions for AWs. So far AWs have been revealed from systems slightly beyond Hopf bifurcation or some other instabilities, and from some wave sources with certain restricted frequencies. Here we study general oscillatory media (including generalized complex Ginzburg-Landau systems and Brusselator model) and specify the parameter conditions of AWs by certain characteristic behaviors of the dispersion relation of the systems. Moreover, we predict that AWs and NWs (normal waves with positive phase velocity) can be realized at a same intrinsic parameter values but different pacing frequencies in parameter regions where the dispersion relation exhibits a maximum or minimum. All numerical simulations are perfectly consistent with these theoretical predictions where the oscillatory systems are driven by external periodic pacings with 1:1 frequency locking responses.

DOI: 10.1103/PhysRevE.80.036211 PACS number(s): 05.45.−a, 47.54.−r, 04.30.Nk

I. INTRODUCTION

Recently, the topic of propagating waves with negative phase velocity has attracted much attention in both fields of linear optics [1–4] and nonlinear oscillatory systems [5–15]. In nonlinear cases, inwardly propagating waves were revealed first in the objects of spiral waves (also target waves) called as antispirals [5,7]. In addition, it has been found that waves propagating toward wave sources can also be generated by external pacing in more general wave forms called simply as antiwaves (AWs) [12–15]. In comparison, we name waves propagating outward from wave sources (with positive phase velocity) as normal waves (NWs). So far most of works on AWs have been based on the complex Ginzburg-Landau equations (CGLE), which are generally valid in nonlinear systems slightly beyond Hopf bifurcations from stationary homogeneous states to homogeneous oscillations. AWs in some reaction-diffusion models have also been investigated in the vicinities of certain Hopf bifurcations in comparison with the corresponding CGLEs [9,13,15]. Moreover, previously all AWs were identified with certain given wave frequencies. Up to date, the question of how to generally distinguish the parameter areas supporting AWs from the areas supporting NWs, without associating to specific pacing frequency or specific bifurcation conditions, has not been clearly and thoroughly answered.

In the present paper we focus on the parameter conditions on which AWs can occur with proper driving frequencies. Throughout the paper, we simplify our discussion to one-dimensional (1D) systems. The paper is organized as follows. In Sec. II, we consider an arbitrary oscillatory chemical reaction-diffusion systems, and study its dispersion relation in the vicinity of homogeneous oscillation. Based on this analysis, we are able to classify different parameter regions supporting AWs and NWs. In Sec. III, we propose a generalized complex Ginzburg-Landau equation (GCGLE) model which can describe oscillatory media near and far from Hopf bifurcation, including the conventional CGLE as its special case. A satisfactory advantage of GCGLE model is that it is exactly solvable for its propagating wave solution and dispersion relation. We apply the general analysis of Sec. II to this solvable model, and explicitly specify parameter regions for NWs and AWs. In the situation far from Hopf bifurcation we reveal from the dispersion relation that N-AW regions where both NWs and AWs can be realized at a same parameter set by using pacings with different frequencies. In Sec. IV, we study a chemical reaction-diffusion model, Brusselator, of which the dispersion relation is no longer analytically solvable (a restriction for most practical systems). We show how to classify NW, AW, and N-AW regions by using numerical calculation of dispersion relation. The last section includes brief discussion and conclusion on the main results of the present work and the perspective of possible future applications.

II. DISPERSION RELATION ANALYSIS OF NW AND AW REGIONS IN OSCILLATORY CHEMICAL REACTION-DIFFUSION SYSTEMS

Suppose we have a set of reaction-diffusion equations in homogeneous n-dimensional (nD) space

$$\frac{d\mathbf{u}}{dt} = \mathbf{f}(\mathbf{a},\mathbf{u}) + \mathbf{D}\nabla^2\mathbf{u}, \tag{1a}$$

$$\mathbf{u} = (u_1, u_2, \ldots, u_m), \quad \mathbf{f} = (f_1, f_2, \ldots, f_m),$$

$$\mathbf{a} = (a_i, i = 1,2, \ldots, q), \quad \mathbf{D} = (D_{ij})(i,j = 1,2, \ldots, m), \tag{1b}$$

where variables $u_1, \cdots, u_m$ represent chemical concentrations, n and q are space and control parameter dimensions, respectively, and a_i and D_{ij} are reaction and diffusion control

*Corresponding author; ganghu@bnu.edu.cn

parameters, respectively. We assume that Eq. (1) has a stable homogeneous limit cycle solution $\mathbf{u}(\mathbf{r},t)=\mathbf{u}(t)$ of frequency ω_0 (called the bulk frequency). In Eq. (1) and in the following we simplify our discussion to 1D systems and assume that all the diffusion rates D_{ij} are independent of the variable concentrations $\mathbf{u}$. All the following framework is valid for general nD cases. For simplicity, we consider only 1D space throughout the paper.

Here is a general question: if we use an external driving with frequency ω_{in} as the wave source of system (1), and this driving force can successfully generate propagating waves of a same frequency ω, $\omega=\omega_{in}$, then which would the propagating waves be, AWs or NWs? This problem has been answered previously as [9,13,14]

$$\text{NWs: if } \omega\omega_0<0 \quad \text{or} \quad \omega\omega_0>0 \quad \text{and} \quad |\omega|>|\omega_0|, \tag{2a}$$

$$\text{AWs: } \omega\omega_0>0 \quad \text{and} \quad |\omega|<|\omega_0|. \tag{2b}$$

The central task of this paper is to determine the parameter regions of $(\mathbf{a},\mathbf{D})$ supporting AWs and NWs. In order to do so we start from the dispersion relation of propagating waves, which can be expanded by a power series

$$\omega=f(k^2)=\sum_{\nu=0}^{\infty} f_\nu k^{2\nu}, \tag{3a}$$

$$f_0=\omega_0, \tag{3b}$$

with ω and k being the frequency and wave number of the propagating waves, respectively. In Eq. (3a) ω is a function of k^2 because of the second space derivative of the diffusion.

AWs are defined by negative phase velocity of $\frac{\omega}{k}<0$. It is known that states of negative group velocity $\frac{d\omega}{dk}<0$ is unstable and cannot be observed in numerical simulations as well as in experiments. Therefore, we accept only physically meaningful cases of $\frac{d\omega}{dk}>0$ (the critical case of $\frac{d\omega}{dk}$ is not considered here). Now we can reduce

$$\frac{d|\omega|}{dk^2}=\frac{\text{sgn }\omega}{2k}\frac{d\omega}{dk}, \quad \text{sgn }\omega=\begin{cases}1, & \omega>0\\ -1, & \omega<0.\end{cases}$$

Since $\frac{d\omega}{dk}>0$, we conclude $\frac{d|\omega|}{dk^2}>0$ if and only if $\frac{\omega}{k}>0$, while $\frac{d|\omega|}{dk^2}<0$ if and only if $\frac{\omega}{k}<0$. This concludes therefore

$$\text{AWs:}\frac{d|\omega|}{dk^2}<0, \tag{4a}$$

$$\text{NWs:}\frac{d|\omega|}{dk^2}>0. \tag{4b}$$

Equation (4) is valid for classifying AWs and NWs in general oscillatory systems. For relating this criterion to actual system parameters, we now study the dispersion relations for small wave number k, where ω is near the bulk frequency ω_0, and we can approximate Eq. (3a) to

$$\omega\approx\omega_0+f_1k^2. \tag{5}$$

Since $|\omega-\omega_0|$ is also small, we consider in this paper only the situation when ω and ω_0 have the same sign (i.e., $\omega\omega_0>0$). Moreover, since $k^2>0$, we should have $\omega>\omega_0(\omega<\omega_0)$ for positive (negative) f_1 in Eq. (5). Thus $|\omega|>|\omega_0|$ can be observed only for $\omega_0f_1>0$, and $|\omega|<|\omega_0|$ can be observed only for $\omega_0f_1<0$. By jointly considering these facts and conditions Eqs. (2) we come to the conclusion,

$$\text{AWs: for } \omega_0f_1<0, \tag{6a}$$

$$\text{NWs: for } \omega_0f_1>0. \tag{6b}$$

The essential points of Eqs. (6) are the following: First, these results are valid for general oscillatory systems which might be far away from Hopf bifurcation conditions. The only restriction is that the k^2 is small and thus ω is not far from ω_0. Second, the quantities in Eqs. (6) classifying AWs and NWs (i.e., the bulk frequency ω_0 and the dispersion coefficient f_1) are determined totally by the parameters of the autonomous oscillatory system Eqs. (1) (not related to external pacing frequency ω_{in}, or say, frequency ω of propagating waves is not involved), and this is sharply different from the conditions of Eqs. (2) where frequency ω is a necessary quantity in determining AWs and NWs. With Eqs. (6) we conclude that in a reference homogeneous oscillation with fixed bulk frequency ω_0, the phase boundary separating AW and NW regions are clearly $f_1=0$ and $\omega_0=0$ with ω_0 and f_1 being system parameters. In comparison, in all previous works [9,13,14] these boundaries are identified with $\omega=0$ and $k=0$, where ω and k are quantities characterizing propagating waves.

III. NW AND AW PARAMETER REGIONS IN GENERALIZED COMPLEX GINZBURG-LANDAU EQUATIONS

In order to illustrate the above argument, we take the following solvable and spatially one-dimensional oscillatory system as our example:

$$\dot{x}=xg(x^2+y^2)-yh(x^2+y^2)+\frac{\partial^2x}{\partial r^2}-\beta\frac{\partial^2y}{\partial r^2}, \tag{7a}$$

$$\dot{y}=yg(x^2+y^2)+xh(x^2+y^2)+\frac{\partial^2y}{\partial r^2}+\beta\frac{\partial^2x}{\partial r^2}, \tag{7b}$$

where x and y may be linear combinations or even complicated functions of the chemical concentrations u_i, $i=1,\ldots,m$; g and h are real functions of $R^2=x^2+y^2$ which are assumed to be expandable as $g(R^2)=\gamma_0+\gamma_1R^2+\gamma_2R^4+\cdots$, $h(R^2)=\alpha_0+\alpha_1R^2+\alpha_2R^4+\cdots$; r is the space coordinate. Defining complex variable $A=x+iy$, Eq. (7) can be transformed to a GCGLE,

$$\dot{A}(r,t)=A(g(|A|^2)+ih(|A|^2))+(1+i\beta)\nabla^2A. \tag{7c}$$

By specifying $g(|A|^2)=1-|A|^2$, $h(|A|^2)=\alpha_1|A|^2$ we can reduce GCGLE to the conventional CGLE: $\dot{A}(r,t)=A$

$-(1-i\alpha_1)A|A|^2+(1+i\beta)\nabla^2 A$. The conventional CGLE considers oscillatory media near and beyond Hopf bifurcation while GCGLE [Eqs. (7a) and (7b)] allows us to study oscillations far from Hopf bifurcation where some essentially new features may be observed as we will see below.

A satisfactory advantage of Eq. (7) is that the propagating waves and the dispersion relation of the system is exactly solvable. In Eq. (7) a homogeneous periodic oscillation in a closed circle with radium R_0,

$$x^2+y^2=R_0^2, \quad g(R_0^2)=0, \tag{8a}$$

exists in $x-y$ phase plane, which oscillates with bulk frequency

$$\omega_0=h(R_0^2), \tag{8b}$$

and the autonomous homogeneous solution reads

$$x(t)=R_0\sin(\omega_0 t+\phi), \quad y(t)=R_0\cos(\omega_0 t+\phi) \tag{9}$$

with ϕ determined by initial conditions. Considering planar waves with wave number k, the oscillatory circle is modified to

$$x^2+y^2=R_k^2, \quad g(R_k^2)-k^2=0, \tag{10a}$$

and the dispersion relation of Eq. (3a) can be specified to

$$\omega=h(R_k^2)-\beta k^2=h(g^{-1}(k^2))-\beta k^2, \tag{10b}$$

and then the solution of waves reads

$$x(r,t)=R_k\sin(\omega t+kr+\phi), \quad y(r,t)=R_k\cos(\omega t+kr+\phi). \tag{11}$$

Now conditions Eqs. (5) can be specified to

$$\text{AWs: if } h(R_0^2)\left(\frac{h'(R_0^2)}{g'(R_0^2)}-\beta\right)<0, \tag{12a}$$

$$\text{NWs: if } h(R_0^2)\left(\frac{h'(R_0^2)}{g'(R_0^2)}-\beta\right)>0,$$

$$\left(\text{note } \omega_0=h(R_0^2),\ f_1=\frac{h'(R_0^2)}{g'(R_0^2)}-\beta\right) \tag{12b}$$

It is emphasized that Eqs. (7) can include oscillatory media far from Hopf bifurcation condition as well as it takes conventional CGLE as its special case. For instance, they can show coexistence of multiple stable limit cycles which are not allowed in the vicinity of a Hopf bifurcation. Equations (8)–(12) are then valid disregarding the distance from a Hopf bifurcation. However, there is a restriction that they are valid for ω not far from the bulk frequency ω_0 of the reference homogeneous oscillations.

We study further some special cases of Eqs. (7), and compare our analytical predictions of Eqs. (12) with numerical simulations.

Example (i).

$$g(x^2+y^2)=1-(x^2+y^2), \quad h(x^2+y^2)=\alpha_1(x^2+y^2). \tag{13}$$

This is exactly the case of conventional CGLE. Now we have $R_0=1$, $R_k=\sqrt{1-k^2}$, leading to

$$\omega=\alpha_1-(\alpha_1+\beta)k^2, \tag{14a}$$

$$\text{AWs: } -\alpha_1(\alpha_1+\beta)<0, \tag{14b}$$

$$\text{NWs: } -\alpha_1(\alpha_1+\beta)>0. \tag{14c}$$

Note in Eq. (14b), we conclude that we observe only AWs for $\beta=0$ (identical diffusion rates of chemical components). Though this conclusion seems to be strange, it is correct for the amplitude equation CGLE. However, it is usually not correct for original oscillatory media Eq. (1) because in deriving CGLE a large eigenfrequency of the Hopf bifurcation ω_h has been removed by the transformation to amplitude equation ($A\to Ae^{i\omega_h t}$). Nevertheless, this original eigenfrequency should be taken into account in determining AWs and NWs in Eq. (2). Introducing α_0 in Eq. (7), we can include this bulk frequency and correctly predict NW and AW regions in original oscillatory systems. Namely, the slightly modified form of CGLE $\frac{\partial A}{\partial t}=(1+i\alpha_0)A-(1+i\alpha_1)|A|^2A+(1+i\beta)\nabla^2 A$ can correctly classify NW and AW parameter regions at $\beta=0$ by including this eigenfrequency at Hopf bifurcation.

Example (ii).

$$g(x^2+y^2)=1-(x^2+y^2),$$

$$h(x^2+y^2)=\alpha_0+\alpha_1(x^2+y^2), \quad \beta=0. \tag{15}$$

Under the conditions of Eq. (15), Eqs. (7) do not contain diffusion dispersion ($\beta=0$), but include both linear and nonlinear circulations ($\alpha_0\neq 0$, $\alpha_1\neq 0$). Then we have $R_0=1$, $R_k=\sqrt{1-k^2}$, leading to

$$\omega=(\alpha_0+\alpha_1)-\alpha_1 k^2, \tag{16a}$$

$$\text{AWs: } -(\alpha_0+\alpha_1)\alpha_1<0, \tag{16b}$$

$$\text{NWs: } -(\alpha_0+\alpha_1)\alpha_1>0. \tag{16c}$$

A prediction in Eqs. (15) and (16) is that both AWs and NWs can be observed in oscillatory systems, which have unit diffusion matrix (without diffusion dispersion). Moreover this classification is determined by different combinations of α_0 and α_1. This agrees with the rich behaviors of practical oscillatory media.

Example (iii).

$$g(x^2+y^2)=-2+3(x^2+y^2)-(x^2+y^2)^2,$$

$$h(x^2+y^2)=\alpha_0+\alpha_1(x^2+y^2). \tag{17}$$

This model is much more complicated than models (13) and (15). First, model (17) is bistable. It has a stable fixed point $R^2=x^2+y^2=0$, and a stable limit cycle $R^2=2$. That is quite not the case in the vicinity of Hopf bifurcation. Moreover the two stable solutions are separated by an unstable limit cycle $R^2=1$. Our study focuses on the reference oscillatory state of $R_0=\sqrt{2}$. Numerically, we drive the system with the initial stable homogeneous oscillation from the left boundary of the

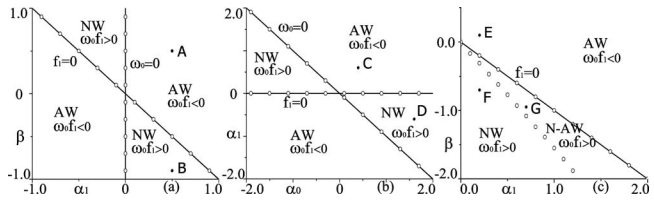

FIG. 1. Distributions of parameter regions for NW, AW, and N-AW motions of Eqs. (7). N-AW region is the parameter domain where both NWs and AWs can be produced at a same parameter set by driving the system with $|\omega|>|\omega_0|$ and $|\omega|<|\omega_0|$, respectively. In comparison, in NW (AW) region we can observe NWs (AWs) with $|\omega|>|\omega_0|$ ($|\omega|<|\omega_0|$) only. ω is the frequency of propagating waves and ω_0 is the frequency of homogeneous oscillation. Solid lines are theoretical predictions of the boundaries of $f_1=0$ and $\omega_0=0$; circles are numerical plots of Eq. (19). In this and all the following figures for Eq. (19) we always take $F=2.0$. Numerical results coincide with the theoretical predictions. (a) Model (13) computed. (b) Model (15) computed. (c) Model (17) computed with $\alpha_0=0.6$. In all Figs. 1–5 numerical simulations are made in 1D space with L=300 space size. Pacing is applied at the left boundary of the 1D medium. Time step $\Delta t=0.0025$ and space step $\Delta r=0.5$ are used for Runge-Kutta 4 algorithm with no-flux boundary condition. In addition, as long as the system is fully driven by pacing, the propagating wave frequency ω is equal to the pacing frequency ω_{in}, $\omega=\omega_{in}$.

1D chain with frequency ω_{in}, and we consider only the case that the system has 1:1 response ($\omega=\omega_{in}$) to the driving. Around the reference oscillation we have $R_0=\sqrt{2}$, $R_k^2=\frac{3+\sqrt{1-4k^2}}{2}$, and

$$\omega = \alpha_0 + \alpha_1 \frac{3+\sqrt{1-4k^2}}{2} - \beta k^2$$

$$= (\alpha_0 + 2\alpha_1) + f_1 k^2 + f_2 k^4 + \cdots,$$

$$f_1 = -(\beta + \alpha_1), \quad f_2 = -2\alpha_1. \tag{18a}$$

Second, the dispersion relation Eq. (18a) is nonlinear with respect to k^2 [it is linear in both Eqs. (14a) and (16a)], and we will find later that this nonlinearity can cause some interesting new features around $f_1=0$. Considering Eqs. (18a) and (5), we predict

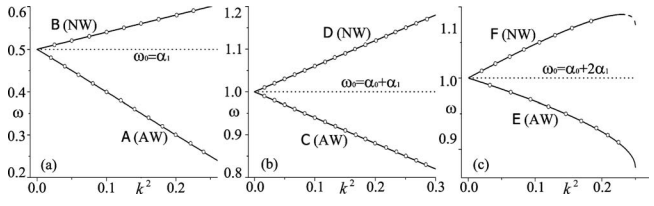

FIG. 2. Theoretical (solid lines) and numerical (circles) results of dispersion lines of Eqs. (7). The circles are numerated by taking Eq. (19). (a) Model (13), A and B sets in Fig. 1(a); (b) Model (15), C and D sets in Fig. 1(b); (c) Model (17), E and F sets in Fig. 1(c). Solid and dashed lines are theoretical predictions of Eqs. (14a), (16a), and (18a) for (a), (b), and (c), respectively. The dashed line in (c) indicates NWs with negative group velocity ($\frac{d\omega}{dk}<0$) which cannot be observed numerically.

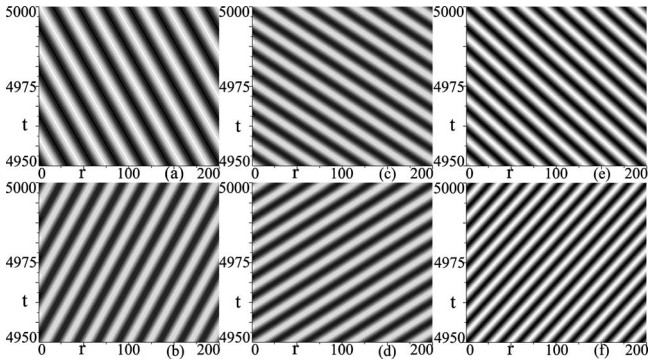

FIG. 3. Time-space patterns of AWs and NWs numerically computed from Eq. (19) by taking the parameter sets in Fig. 1. The gray scale shows the numerical value of variable y (dark for small y and light for large y). (a) AWs with $k^2=0.05$, A ($\alpha_1=0.5$, $\beta=0.5$, $\omega=\omega_{in}=0.45$); (b) NWs with $k^2=0.075$, B ($\alpha_1=0.5$, $\beta=-0.9$, $\omega=\omega_{in}=0.53$); (c) AWs with $k^2=0.033$, C ($\alpha_0=0.4$, $\alpha_1=0.6$, $\omega=\omega_{in}=0.98$); (d) NWs with $k^2=0.033$, D ($\alpha_0=1.6$, $\alpha_1=-0.6$, $\omega=\omega_{in}=1.02$); (e) AWs with $k^2=0.064$, E ($\alpha_0=0.6$, $\alpha_1=0.2$, $\beta=0.1$, $\omega=\omega_{in}=0.98$); (f) NWs with $k^2=0.10$, F ($\alpha_0=0.6$, $\alpha_1=0.2$, $\beta=-0.7$, $\omega=\omega_{in}=1.05$), respectively. Parameter sets A, B, C, D, E, and F are marked in Fig. 1. These patterns coincide with the classifications of motion types in Fig. 1.

$$\text{AWs:} \quad -(\alpha_0 + 2\alpha_1)(\alpha_1 + \beta) < 0, \tag{18b}$$

$$\text{NWs:} \quad -(\alpha_0 + 2\alpha_1)(\alpha_1 + \beta) > 0. \tag{18c}$$

In Eqs. (14), (16), and (18) the quantity of wave frequency ω does not enter into the conditions distinguishing AWs and NWs, unlike conditions Eqs. (2). This indicates that Eqs. (14), (16), and (18) give the parameter regions necessary for AWs and NWs, where all proper pacing frequencies can successfully generate traveling waves in the given media.

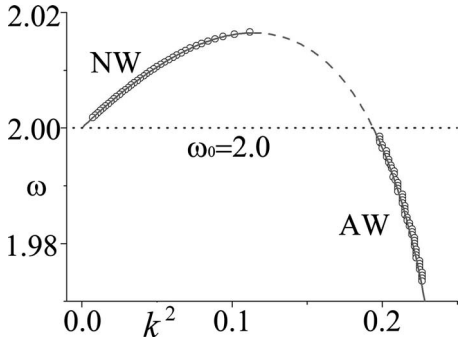

FIG. 4. Analytical and numerical dispersion-relation lines of system (17) with $\alpha_0=0.6$, $\alpha_1=0.7$, $\beta=-0.95$ [parameter set G in Fig. 1(c) in the N-AW region]. In the segments NW and AW, numerical results are consistent with the theoretical predictions of Eqs. (18a) and (21b). The dashed line represents negative group velocity [Eq. (21b) describes approximately this interval], and the corresponding waves are not numerically observed.

For numerically producing propagating waves we simulate 1D chain of Eq. (7) with periodical pacing at the left boundary ($r=0$) as

$$\dot{A}(r,t) = A(g(|A|^2) + ih(|A|^2)) + (1+i\beta)\nabla^2 A + \delta(r)Fe^{i\omega_{in}t}. \tag{19}$$

In Figs. 1(a)–1(c) we plot both theoretical and numerical results of AW and NW regions in parameter planes of Eqs. (13), (15), and (17), respectively. In these figures numerical simulations are well consistent with the predictions of parameter regions supporting AWs and NWs. The theoretically predicted and numerically computed dispersion relations of the parameter sets A,B; C,D; and E,F shown in Fig. 1 are presented in Figs. 2(a)–2(c), respectively. Again direct numerical computations of Eq. (19) agree with the theoretical predictions for all three models (13), (15), and (17). The time-space behaviors of AWs and NWs with different parameter sets are shown in Fig. 3.

So far in all previous works oscillatory media always have diffusion dispersion or unsymmetrical diffusion matrix when negative phase velocity is observed. In Eq. (15) we predict for the first time that AWs may appear in oscillatory systems without diffusion dispersion ($\beta=0$) while $\alpha_0+\alpha_1$ and α_1 have the same sign. All numerical results of Figs. 1(b), 2(b), and 3(c) support this theoretical analysis.

Conclusions Eqs. (6) are exact if the linear dispersion relation Eq. (5) is exactly valid. Moreover this is the case of Eqs. (14a) and (16a), leading to the distributions of Figs. 1(a) and 1(b), where AW and NW regions are clearly separated by the condition $f_1=0$. Generally, high orders of k^2 exist in the dispersion relation, as we see in Eq. (18a). These nonlinear k^2 terms lead to some new features, of which the existence of N-AW region in Fig. 1(c) is the most interesting one. In this region, both NWs and AWs can be observed in the medium at a same parameter set by taking pacing with different frequencies. This is a typical behavior far from Hopf bifurcation. In the parameter region around $f_1=0$, high orders of k^2 can play role in determining propagating waves. Suppose $|f_1| \ll 1$ while $f_2 \neq 0$ in expansion Eq. (3), we can replace the approximation Eq. (5) by

$$\omega \approx \omega_0 + f_1 k^2 + f_2 k^4 \tag{20}$$

for the leading terms. Equation (20) can be solved as

$$\omega_0 f_1 > 0, \quad \omega_0 f_2 > 0 : |\omega| - |\omega_0| > 0 \text{ NWs},$$

$$\omega_0 f_1 > 0, \quad \omega_0 f_2 < 0 : |\omega| - |\omega_0| > 0 \quad \text{for } k^2 \lesssim -\frac{f_1}{2f_2} \text{ NWs}, \tag{21a}$$

$$|\omega| - |\omega_0| < 0 \quad \text{for } k^2 \gtrsim -\frac{f_1}{f_2} \text{ AWs},$$

$$-\frac{f_1}{2f_2} < k^2 < -\frac{f_1}{f_2} \text{ unobservable waves with group velocity } v_g < 0, \tag{21b}$$

$$\omega_0 f_1 < 0, \quad \omega_0 f_2 < 0 : |\omega| - |\omega_0| < 0 \text{ AWs},$$

$$\omega_0 f_1 < 0, \quad \omega_0 f_2 > 0 : |\omega| - |\omega_0| < 0 \quad \text{for } k^2 \lesssim -\frac{f_1}{2f_2} \text{ AWs}, \tag{21c}$$

$$|\omega| - |\omega_0| > 0 \quad \text{for } k^2 \gtrsim -\frac{f_1}{f_2} \text{ NWs},$$

$$-\frac{f_1}{2f_2} < k^2 < -\frac{f_1}{f_2} \text{ unobservable waves with group velocity } v_g < 0, \tag{21d}$$

where $v_g = \frac{d\omega}{dk}$ indicates the group velocity of propagating waves.

Note, all analytical predictions of Eqs. (21a)–(21d) are drawn by neglecting the higher orders $\Sigma_{\nu=3}^{\infty} f_\nu k^{2\nu}$ in the dispersion relation Eq. (3a). Summarizing all results of Eqs. (6) and (21), we conclude the following:

(i) For $\omega_0 f_1 > 0$, we can produce NWs with $|\omega| > |\omega_0|$;
(ii) For $\omega_0 f_1 < 0$, we can produce AWs with $|\omega| < |\omega_0|$;

Around $f_1 \approx 0$, $f_2 \neq 0$, we can generically identify N-AW region where both NWs and AWs can be produced at a same parameter set with wave sources having different frequencies. Precisely, we observe the following:

(iii) For $\omega_0 f_2 > 0$, the NW region invades the boundary of $f_1=0$, and thus the N-AW region appears in the area of $\omega_0 f_1 < 0$;
(iv) For $\omega_0 f_2 < 0$, the AW region crosses the boundary of $f_1=0$, and the N-AW region appears in the area of $\omega_0 f_1 > 0$;

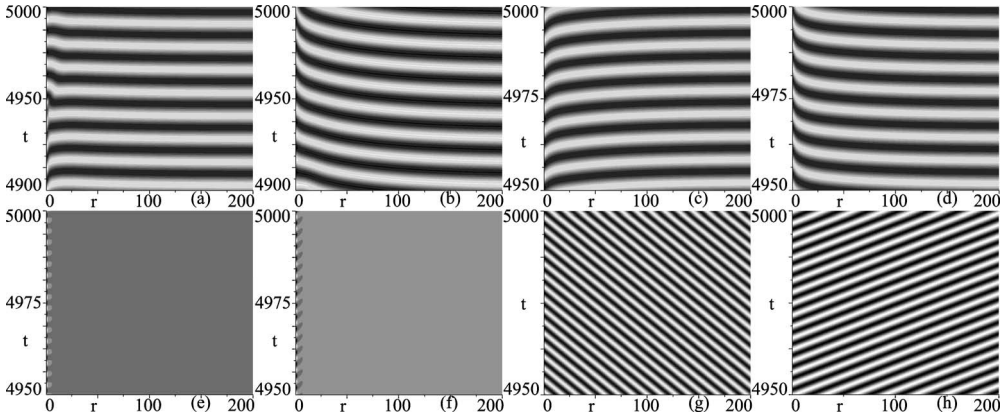

FIG. 5. Numerical results of time-space patterns of Eq. (19) with various driving frequencies in different parameter regions. (a) and (b) for model (13); (c) and (d) for model (15); (e), (f), (g), and (h) for model (17). (a), (c), and (e) In AW regions we cannot produce NWs for the driving $|\omega_{in}|>|\omega|\approx|\omega_0|$: (a) Set A in Fig. 1(a), $|\omega_{in}|=0.53>|\omega|\approx|\omega_0|=0.5$; (c) Set C in Fig. 1(b), $|\omega_{in}|=1.02>|\omega|\approx|\omega_0|=1.0$; (e) Set E in Fig. 1(c), $|\omega_{in}|=1.05>|\omega|\approx 0$. (b), (d), and (f) In NW regions one cannot produce AWs for $|\omega_{in}|<|\omega|\approx|\omega_0|$: (b) Parameter set B in Fig. 1(a), $|\omega_{in}|=0.45<|\omega|\approx|\omega_0|=0.5$; (d) Set D in Fig. 1(b), $|\omega_{in}|=0.98<|\omega|\approx|\omega_0|=1.0$; (f) Set F in Fig. 1(c), $|\omega_{in}|=0.98>|\omega|\approx 0$. (g), (h) Set G in Fig. 1(c). In N-AW region one can successfully produce both AWs and NWs at a same parameter set: (g) AWs with $|\omega|=|\omega_{in}|=1.99$, $|\omega_0|=2.0$, $k^2\approx 0.0529$ and (h) with NWs $|\omega|=|\omega_{in}|=2.01$, $|\omega_0|=2.0$, $k^2\approx 0.0277$.

In both cases (iii) and (iv) N-AW region appears for $f_1 f_2<0$.

(v) The N-AW parameter domain ends at the parameter condition where the wave number $k^2(\omega=\omega_0)\approx-\frac{f_1}{f_2}$ is too large that waves with $k^2\gtrsim k^2(\omega=\omega_0)$ can no longer be supported by the medium. This condition determines the left-low boundary of the N-AW domain in Fig. 1(c). However, there is no analytical precise prediction available for this phase boundary so that it can be determined only numerically.

All the above points are concluded based on the general expansion of dispersion relation Eq. (20), and numerical results in Fig. 1(c) are consistent with these theoretical analysis. Since nonlinear $|\omega|-k^2$ dispersion relations exist generally, the distributions of Fig. 1(c) is expected to be general in realistic oscillatory systems, while Figs. 1(a) and 1(b) (without N-AW region) are observed only for particular systems of probability zero. In Fig. 4 we plot the dispersion relation of Eq. (18a) at the parameter set of G in Fig. 1(c). Solid curve represents the theoretical prediction Eq. (18a) while circles are plotted by numerical simulation of Eq. (19). It is obvious that numerical results coincide with theoretical predictions. Numerical computation cannot produce the dashed segment in Fig. 4 because in this part waves have negative group velocity v_g, they are unstable and thus numerically unobservable. In Fig. 5 we present various spatiotemporal patterns of waves in NW, AW, and N-AW regions, and all the predictions of Eqs. (21) are numerically observed.

IV. PARAMETER REGIONS SUPPORTING NWS AND AWS IN BRUSSELATOR

For Eqs. (7) the dispersion relation is explicitly computable. However, for general chemical reaction-diffusion systems analytic results of dispersion relation are not available. Nevertheless, we can numerically compute the dispersion relation, and examine the theory of Eqs. (4) [or equivalently Eqs. (6)]. Let us consider a chemical reaction-diffusion model, Brusselator, which has been investigated extensively [9,12,13],

$$\dot{u}=a-(1+b)u+u^2v+\nabla^2u+\delta(r)F\sin(\omega_{in}t), \quad (22a)$$

$$\dot{v}=bu-u^2v+\delta\nabla^2v+\delta(r)F\cos(\omega_{in}t), \quad (22b)$$

where u and v are concentrations of two chemical variables. We consider a 1D medium in the physical space $[0,L]$, and adopt no-flux boundary condition. A periodic pacing is applied to the left boundary of the medium. For $b>1+a^2$, system (22) has a stable homogeneous limit cycle solution when $F=0$. By applying nonzero F, characteristically different wave solutions can be generated at different sets of parameters. The parameter regions can be classified to three types: AW, NW, and N-AW regions, similar to those in Fig. 1(c).

We apply Runge-Kutta 4 algorithm for numerical simulations and use $\Delta t=0.0025$, $\Delta r=0.5$ for time and space discreteness, $F=2.0$. The correctness of all the following results have been justified by varying the time and space steps. In Fig. 6(a) we fix $a=1.0$, $b=3.2$, $\delta=0.5$ and plot the output frequency ω [i.e., the frequency of variables $u(t)$ and $v(t)$ in space region far away from the point being paced] against the pacing frequency ω_{in}. It is shown that in an ω_{in} interval $(0.843<\omega_{in}<1.111)$, we have $\omega=\omega_{in}$, which is called 1:1 driven region. In this region the system is fully driven by the pacing. In the following we study the behaviors of NWs and AWs in this 1:1 driven region $(\omega=\omega_{in})$ only. In Fig. 6(b) we plot $|\omega|$ against the square of wave number k^2 within the 1:1 parameter region of Fig. 6(a). We find that $|\omega|$ increases monotonously against k^2. This behavior satisfies condition of Eq. (4b), and we thus predict NWs in this domain. In Fig. 6(c) we use pacing frequency of point P in Fig. 6(b) and plot the time-space pattern for the asymptotic waves which are clearly NWs. For Figs. 6(d)–6(f) we do exactly the same computation as we do for Figs. 6(a)–6(c), respectively, with

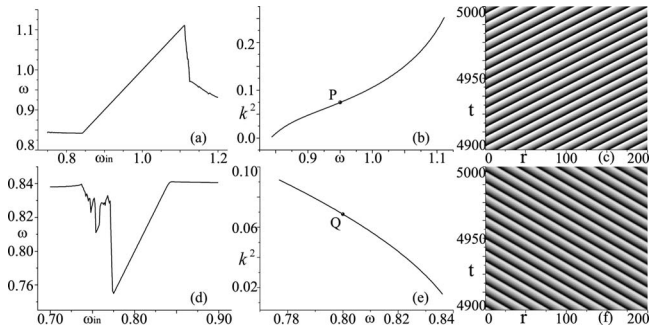

FIG. 6. Numerical results of AW, and NW waves for 1D Brusselator model Eqs. (22). Periodic driving is applied at the left boundary ($r=0$). $\Delta t=0.0025$ and $\Delta r=0.5$ for Runge-Kutta 4 algorithm with no-flux boundary condition. (a), (b), and (c) $a=1.0$, $b=3.2$, $\delta=0.5$. (a) ω vs ω_{in}. 1:1 response ($\omega=\omega_{in}$) is observed in the interval $0.843<\omega_{in}<1.111$. (b) k^2 vs $|\omega|$ in the 1:1 response interval. Monotonous increasing tendency is observed, and NWs are expected. (c) NWs are numerically produced by the driven frequency $\omega=\omega_{in}=0.95$ [point P in (b)]. $k^2\approx 0.075$. (d), (e), and (f) The same as (a), (b), and (c), respectively, with parameter set changed to $a=1.0$, $b=3.2$, $\delta=2.5$. (d) A 1:1 driven region appears in $0.775<\omega_{in}<0.839$. (e) Monotonous decreasing dispersion relation is observed in the 1:1 driven region, and AWs are expected in this parameter interval. In (f) we use $\omega=\omega_{in}=0.80$ [point Q in (e)], and AWs are observed, with $k^2\approx 0.068$. (c), (f) The gray scale shows the numerical value of variable v (dark for small v and light for large v).

parameters replaced by $a=1.0$, $b=3.2$, $\delta=2.5$. At this parameter set we can also identify 1:1 region of ω/ω_{in} in Fig. 6(d) ($0.775<\omega_{in}<0.839$). In Fig. 6(e) we find that in this 1:1 driven region $|\omega|$ decreases with k^2, indicating condition Eq. (4a) and predicting AWs. Indeed, we find numerically negative phase velocity in Fig. 6(f) by taking ω_{in} at point Q in Fig. 6(e).

For system Eqs. (22) we cannot give analytical dispersion form and cannot theoretically predict the parameter regions for NWs, AWs, or N-AWs. However, with numerical computation of dispersion relation we can specify the distributions of parameter regions with different characteristic motions. In Fig. 7(a) we plot AW, NW, and N-AW regions in $b-\delta$ parameter plane with $a=1.0$. In NW (AW) region we can identify a finite interval of 1:1 ω/ω_{in} driven region like Fig. 6(a) [Fig. 6(d)] where monotonously increasing (decreasing) $|\omega|-k^2$ curve is explored as Fig. 6(b) [Fig. 6(e)], and thus NWs (AWs) can be observed as Fig. 6(c) [Fig. 6(f)]. In the N-AW region, both AWs and NWs of frequency $\omega=\omega_{in}$ can be generated by pacings with different frequencies $\omega_{in}<\omega_0$ and $\omega_{in}>\omega_0$, respectively. This feature is exactly the same as that shown in Fig. 1(c). In Fig. 7(b) we fix $b=3.2$, and specify 1:1 AW and NW regions by varying parameter δ along the dotted line in Fig. 7(a) and by changing the pacing frequency ω_{in}. Unlike Fig. 7(a), where AW and NW regions overlap in the N-AW parameter region in $b-\delta$ plane, in Fig. 7(b) AW and NW regions are always separated in $\delta-\omega$ plane. However, the δ interval of AWs enters the region of NWs (though with different frequencies), and this is just the characteristic of N-AW region.

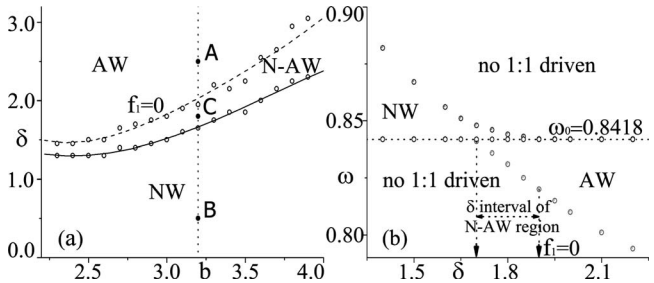

FIG. 7. (a) Distributions of AW, NW, and N-AW regions of Eqs. (22) in $b-\delta$ parameter plane. Circles are numerical results, and continuous curves are fitting lines. The dashed curve $f_1=0$ is judged by Eqs. (21) and verified by direct numerical computation of dispersion curves. (b) $b=3.2$ (the dotted line in (a)). Distribution of AW, NW, and N-AW regions plotted in $\delta-\omega$ plane. In the interval $1.7<\delta<1.9$ we can produce both NWs and AWs at a same δ by using different driving frequencies ($\omega=\omega_{in}>\omega_0>0$ for NWs and $0<\omega=\omega_{in}<\omega_0$ for AWs). The N-AW domain coincides with that in (a).

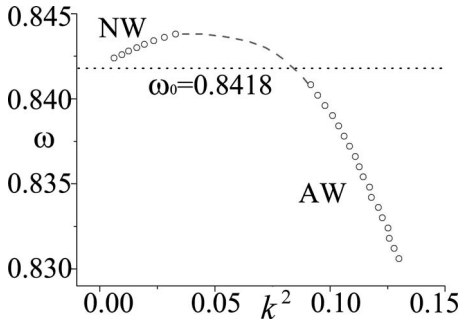

FIG. 8. The same as Fig. 4 with Brusselator Eqs. (22) computed numerically. $a=1.0$, $b=3.2$, $\delta=1.8$. Circles represent numerical data, while dashed line is drawn by smooth fitting with circles.

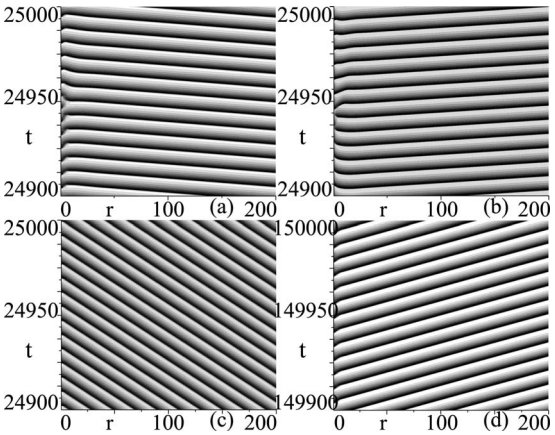

FIG. 9. The same as Fig. 5 with model Eqs. (22) computed. (a) $a=1.0$, $b=3.2$, $\delta=2.5$ [point A in Fig. 7(a)]. $|\omega_{in}|=0.9>|\omega|\approx|\omega_0|=0.8418$ is used in AW region. The system is not driven. (b) $a=1.0$, $b=3.2$, $\delta=0.5$ [point B in Fig. 7(a)]. $|\omega_{in}|=0.8<|\omega|\approx|\omega_0|=0.8418$ is used in NW region. The system is also not driven. (c), (d) $a=1.0$, $b=3.2$, $\delta=1.8$ [point C in Fig. 7(a)]. (c) $|\omega|=|\omega_{in}|=0.84<|\omega_0|$, $k^2\approx 0.0958$. AWs are observed. (d) $|\omega|=|\omega_{in}|=0.843>|\omega_0|$, $k^2\approx 0.0161$. NWs are observed. Coexistence of NWs and AWs are observed only in the N-AW domain, but never in NW or AW region.

In Fig. 8 we do the same computation as for Fig. 4 with model replaced by Eqs. (22), and only numerical data are presented (there is no analytical result available). The dashed line, representing numerically unobservable waves with negative group velocity, is estimated by a smooth continuous fitting to link the NW and AW dispersion segments. From the humped shape of the dispersion curve we judge, based on Eqs. (21), that in Fig. 7(a) $f_1=0$ occurs on the upper boundary of N-AW domain. Moreover AW region slightly crosses the $f_1=0$ boundary, invades the domain of $\omega_0 f_1>0$, where the high orders of k^2 terms of the dispersion relation play role in producing AWs, as we predicted in Eq. (21b). In Fig. 9 we do the same computation as for Fig. 5 with model Eqs. (22). We show that in the N-AW domain we can produce both NWs and AWs with a same parameter set C in Fig. 7(a) by taking different pacing frequencies ($|\omega_{in}|<|\omega_0|$ for AWs [Fig. 9(c)] and $|\omega_{in}|>|\omega_0|$ for NWs [Fig. 9(d)]). However, in NW and AW domains we can produce only NWs for set B and AWs for set A, but not both. With $|\omega_{in}|>|\omega_0|$ in AW region and $|\omega_{in}|<|\omega_0|$ in NW region, we can only get waves with a frequency ω far away from the pacing frequency ω_{in} ($\omega\neq\omega_{in}$) but close to the bulk frequency ω_0 ($\omega\approx\omega_0$) [Figs. 9(a) and 9(b)]. These behaviors are precisely the same as those in Figs. 5(a)–5(d). These numerical observations are again consistent with the theoretical predictions of Eqs. (21). They show the robustness of the features in Fig. 1(c) for general oscillatory systems with nonlinear $|\omega|-k^2$ dispersion curves. It is obvious that in all cases tested (i.e., in all AW, NW, and N-AW regions) $|\omega|$ is always larger (smaller) than $|\omega_0|$ for NWs (AWs). These observations agree with the previous conclusions of Eqs. (2) [9,13,14].

V. CONCLUSION

In conclusion we have defined parameter conditions supporting NWs and AWs in general oscillatory systems, based on the analysis of dispersion relations. The validity of the conditions is not related to special source frequency and not restricted to the vicinity of Hopf bifurcations nor other wave instabilities. Numerical computations are consistent with the theoretical predictions. Moreover, we found a parameter domain around the vicinity of the turning boundary $f_1=0$ where periodic pacing can produce both AWs and NWs but with different driving frequencies at a same autonomous parameter set. All the results in this paper clearly show where and how one can observe waves with negative phase velocity, and this can help experimentalists to produce AWs in practical.

ACKNOWLEDGMENTS

This work was supported by the National Natural Science Foundation of China under Grant No. 10675020 and the National Basic Research Program of China, 973 Program, under Grant No. 2007CB814800.

[1] V. G. Veselago, Sov. Phys. Usp. **10**, 509 (1968).
[2] R. A. Shelby, D. R. Smith, and S. Schultz, Science **292**, 77 (2001).
[3] C. G. Parazzoli, R. B. Greegor, K. Li, B. E. C. Koltenbah, and M. Tanielian, Phys. Rev. Lett. **90**, 107401 (2003).
[4] D. R. Smith, J. B. Pendry, and M. C. K. Wiltshire, Science **305**, 788 (2004).
[5] V. K. Vanag and I. R. Epstein, Science **294**, 835 (2001).
[6] V. K. Vanag and I. R. Epstein, Phys. Rev. Lett. **88**, 088303 (2002).
[7] L. Yang, M. Dolnik, A. M. Zhabotinsky, and I. R. Epstein, J. Chem. Phys. **117**, 7259 (2002).
[8] Y. Gong and D. J. Christini, Phys. Rev. Lett. **90**, 088302 (2003); Phys. Lett. A **331**, 209 (2004).
[9] L. Brusch, E. M. Nicola, and M. Bär, Phys. Rev. Lett. **92**, 089801 (2004); E. M. Nicola, L. Brusch, and M. Bär, J. Phys. Chem. B **108**, 14733 (2004).
[10] P. J. Kim, T. W. Ko, H. Jeong, and H. T. Moon, Phys. Rev. E **70**, 065201(R) (2004).
[11] C. Wang, C. X. Zhang, and Q. Ouyang, Phys. Rev. E **74**, 036208 (2006).
[12] R. Zhang, L. Yang, A. M. Zhabotinsky, and I. R. Epstein, Phys. Rev. E **76**, 016201 (2007).
[13] Z. Cao, H. Zhang, and G. Hu, EPL **79**, 34002 (2007).
[14] Z. Cao, P. Li, H. Zhang, and G. Hu, Int. J. Mod. Phys. B **21**, 4170 (2007).
[15] X. Shao, Y. Wu, J. Z. Zhang, H. L. Wang, and Q. Ouyang, Phys. Rev. Lett. **100**, 198304 (2008).